

Mitigation of Voltage Dips Through Distributed Generation Systems

Koen J. P. Macken, *Member, IEEE*, Math H. J. Bollen, *Senior Member, IEEE*, and
Ronnie J. M. Belmans, *Senior Member, IEEE*

Abstract—Voltage dips are often responsible for disrupting the operation of sensitive electronic equipment. In this paper, two solutions are presented to prevent sensitive equipment from disruptive operation. Both solutions make use of distributed generation systems to maintain the voltage across the equipment in the presence of voltage dips. The emphasis of this paper is on the transient response of both solutions to balanced as well as unbalanced voltage dips. Simulations have been carried out to provide a thorough analysis.

Index Terms—Distributed generation, microgrid operation, power electronic converter, power quality, series compensation, voltage dips.

I. INTRODUCTION

VOLTAGE DIPS have been forming a serious power quality problem for many years [1]–[3]. Voltage dips are short-duration reductions (between 10%–90%) in voltage magnitude, lasting from one-half cycle to several seconds. They occur due to faults, motor starting, and energizing of transformers. Electronic equipment is very sensitive to voltage dips. Computers, adjustable-speed drives, and process-control equipment, for example, frequently trip as a consequence of a dip in voltage.

Two solutions are suggested here to protect sensitive equipment against voltage dips. In both solutions distributed generation systems play an important role. It is expected that distributed generation from, e.g., wind energy, microturbines, fuel cells, etc., will grow in the coming years as a consequence of the heightened awareness of environmental issues in combination with the restructuring of the electric industry.

One solution is to extend a power electronic converter, used to grid connect a distributed generation system, with a series compensator. The series compensator is able to restore the voltage at the load side in case of a voltage dip.

Another solution is to transfer a particular part of the power system, where sensitive equipment is located, to microgrid operation during a dip. A static transfer switch is used to isolate

Paper ICPSD-03IAS30-4, presented at the 2003 Industry Applications Society Annual Meeting, Salt Lake City, UT, October 12–16, and approved for publication in the IEEE TRANSACTIONS ON INDUSTRY APPLICATIONS by the Power Systems Engineering Committee of the IEEE Industry Applications Society. Manuscript submitted for review October 15, 2003 and released for publication July 15, 2004.

K. J. P. Macken and R. J. M. Belmans are with the Department of Electrical Engineering, Katholieke Universiteit Leuven, B-3001 Leuven, Belgium (e-mail: koen.macken@ieee.org; ronnie.belmans@esat.kuleuven.ac.be).

M. H. J. Bollen was with the School of Electrical Engineering, Chalmers University of Technology, SE-412 96 Gothenburg, Sweden. He is now with STRI AB, SE-771 80 Ludvika, Sweden (e-mail: math.bollen@stri.se).

Digital Object Identifier 10.1109/TIA.2004.836302

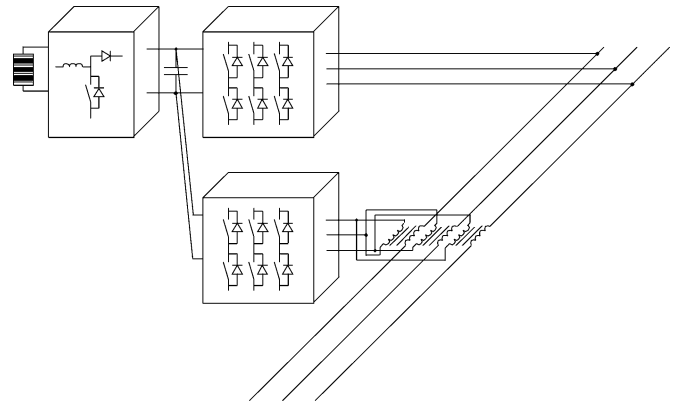


Fig. 1. A grid-interfaced distributed generation system extended with a series compensator.

that particular part of the system from the utility supply. During microgrid operation the voltage is controlled by the distributed generation system(s) [4], [5].

The aim of this paper is to compare the transient performance of both solutions. In Section II, the series compensation of voltage dips is treated in more detail. Section III deals with the transfer to microgrid operation during voltage dips. In Section IV, the detection of dips is briefly addressed. The transient performance is analyzed in Section V. Finally, the conclusion is given in Section VI.

II. SERIES COMPENSATION

Mitigation of voltage dips is possible by injecting either a shunt current or a series voltage. Although shunt injection can be easily achieved with the power electronic converter of a distributed generation system, it requires a high active current if the voltage has to be restored in both magnitude and phase angle to its pre-fault values. Series compensation requires considerably less active power and is, therefore, chosen here. This demands, however, a voltage-source inverter that has to be connected in series with the grid [6]–[8].

The power electronic converter of a distributed generation system can be extended with a series compensator as shown in Fig. 1. An additional voltage-source inverter is connected to the dc bus of the distributed generation system. A transformer is used to connect the output of the voltage-source inverter in series with the grid. In this way, it is possible to inject a voltage in series with the supply voltage when a dip occurs.

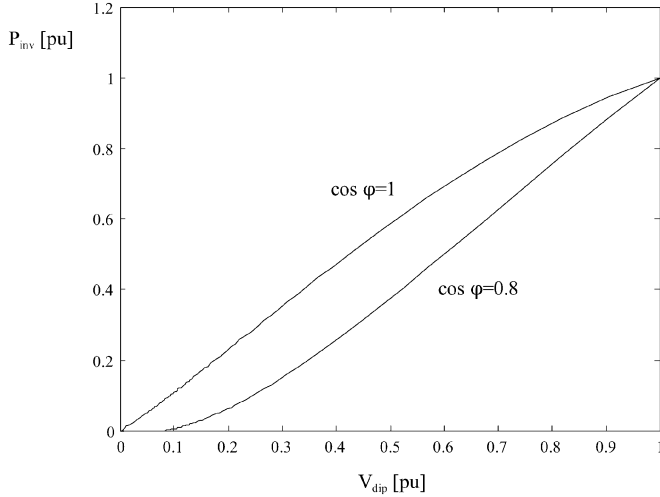


Fig. 2. Required active power as a function of voltage dip magnitude for two load power factors.

The active power required for the series-connected inverter P_{inv} to compensate for a three-phase balanced voltage dip V_{dip} can be expressed as [9]

$$P_{inv} = \left[\frac{1 - (1 - V_{dip}) \cos(\varphi + \psi)}{\cos \varphi} \right] P_{load} \quad (1)$$

where ψ is phase-angle jump, φ is load angle, and P_{load} is total active power of the load.

Voltage dip magnitude and phase-angle jump can be calculated from

$$1 - \vec{V}_{dip} = \frac{\lambda}{\lambda + e^{j\alpha}} \quad (2)$$

where λ is a measure of the electrical distance, and α is impedance angle.

The active power requirement as a function of voltage dip magnitude for two load power factors is shown in Fig. 2. An impedance angle of $\alpha = -60^\circ$ is taken, while λ varies between zero and infinite. An impedance angle of -60° corresponds to the largest phase-angle jumps that occur in practice. The range of λ covers all values of the retained voltage during the dip (dip magnitude). Further, the active load power is 1 pu. Thus, in order to compensate for a voltage dip of, e.g., 0.3 pu, the series compensator requires 0.15 pu active power when the power factor is 0.8. Note that (1) was derived by keeping the active part of the load power constant, so that the load current increases for a decreasing power factor. This is discussed in more detail in [9]. It is important to note that the voltage tolerance is not affected by the dip duration, since the power required for the compensation is provided by the distributed generation source.

In order to effectively mitigate voltage dips, a controller with a fast dynamic response is required. The average model of the series compensator, as shown in Fig. 3, is used to design the controller. This model describes the behavior of the inverter for average values of voltage and current without switching ripple [10], [11]. In this figure, v_a , v_b , and v_c are the average output voltages of the inverter and i_a , i_b , and i_c are the corresponding average output currents. The inverter output is connected through an LC filter, which is not shown in Fig. 1, with the se-

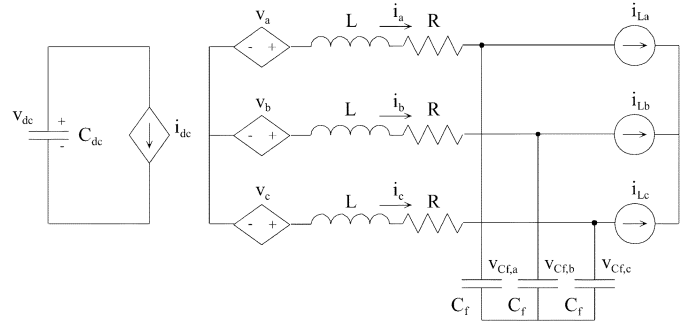


Fig. 3. Average model of a three-phase series-connected voltage-source inverter with LC filter.

ries transformer. The inductors of this filter have an inductance L and a resistance R . The capacitance of the capacitors is C_f . The voltages across the capacitors are denoted by v_{Cfa} , v_{Cfb} , and v_{Cfc} for phases a , b , and c , respectively. The turns ratio of the transformer is 1 : 1. Both transformer and load are replaced by ideal current sources, i.e., i_{La} , i_{Lb} , and i_{Lc} . The dc input of the inverter is modeled as a controlled current source i_{dc} , where the dc-bus voltage is kept constant at v_{dc} . The dc-bus capacitor has a capacitance C_{dc} .

From Fig. 3, the differential equations in state-space notation describing the dynamics of the model are found. When represented in a dq reference frame, these equations are

$$\begin{aligned} \dot{x}(t) &= Ax(t) + Bu(t) + Ew(t) \\ y(t) &= Cx(t) \end{aligned} \quad (3)$$

where system, control, disturbance, and output matrices, respectively, are

$$\begin{aligned} A &= \begin{bmatrix} 0 & \omega & \frac{1}{C_f} & 0 \\ -\omega & 0 & 0 & \frac{1}{C_f} \\ \frac{-1}{L} & 0 & \frac{-R}{L} & \omega \\ 0 & \frac{-1}{L} & -\omega & \frac{-R}{L} \end{bmatrix} \\ B &= \begin{bmatrix} 0 & 0 \\ 0 & 0 \\ \frac{1}{L} & 0 \\ 0 & \frac{1}{L} \end{bmatrix} \\ E &= \begin{bmatrix} \frac{-1}{C_f} & 0 \\ 0 & \frac{-1}{C_f} \\ 0 & 0 \\ 0 & 0 \end{bmatrix} \\ C &= \begin{bmatrix} 0 & 0 & 1 & 0 \\ 0 & 0 & 0 & 1 \end{bmatrix} \end{aligned}$$

and state, control, and disturbance vectors, respectively, are

$$\begin{aligned} x(t) &= [v_{Cfa}(t) \quad v_{Cfb}(t) \quad i_d(t) \quad i_q(t)]^T \\ u(t) &= [v_d(t) \quad v_q(t)]^T \\ w(t) &= [i_{Ld}(t) \quad i_{Lq}(t)]^T. \end{aligned}$$

Equation (3) is used to derive the controller for the series compensator. The purpose of the controller is to regulate the voltage that has to be injected into the grid in order to compensate for the voltage dips. Since the transformer turns ratio is 1 : 1, the injected voltage is equal to the voltage across the capac-

itor and, consequently, the controller has to act on this capacitor voltage. This is done by a cascaded controller, where the outer control loop regulates the capacitor voltage and the inner control loop regulates the current through the inductor. The outer control loop constitutes the reference for the inner control loop. The controller is implemented in discrete time. Discretization of (3) is obtained using a forward difference approximation [12]. The sampling period is T_s . From these discretized equations, the controller equations are derived. In order to achieve a fast dynamic response, both outer and inner control loops are designed to adopt a deadbeat response. Steady-state errors are avoided by including an integral action in the inner control loop.

The outer or voltage control loop is

$$\begin{bmatrix} i_{d,ref}(k) \\ i_{q,ref}(k) \end{bmatrix} = \begin{bmatrix} \frac{C_f}{T_s} & 0 \\ 0 & \frac{C_f}{T_s} \end{bmatrix} \begin{bmatrix} v_{Cfd,ref}(k) - \hat{v}_{Cfd}(k) \\ v_{Cfq,ref}(k) - \hat{v}_{Cfq}(k) \end{bmatrix} + \begin{bmatrix} 0 & -\omega C_f & 1 & 0 \\ \omega C_f & 0 & 0 & 1 \end{bmatrix} \begin{bmatrix} \hat{v}_{Cfd}(k) \\ \hat{v}_{Cfq}(k) \\ i_{Ld}(k) \\ i_{Lq}(k) \end{bmatrix}. \quad (4)$$

Further, the inner or current control loop is

$$\begin{bmatrix} v_{d,ref}(k) \\ v_{q,ref}(k) \end{bmatrix} = \begin{bmatrix} \frac{L}{T_s} + \frac{R}{2} & 0 \\ 0 & \frac{L}{T_s} + \frac{R}{2} \end{bmatrix} \times \begin{bmatrix} i_{d,ref}(k) - \hat{i}_d(k) \\ i_{q,ref}(k) - \hat{i}_q(k) \end{bmatrix} + \begin{bmatrix} 0 & -\omega L & 1 & 0 \\ \omega L & 0 & 0 & 1 \end{bmatrix} \begin{bmatrix} \hat{i}_d(k) \\ \hat{i}_q(k) \\ v_{Cfd,ref}(k) \\ v_{Cfq,ref}(k) \end{bmatrix} + \begin{bmatrix} \xi_d(k) \\ \xi_q(k) \end{bmatrix} \quad (5)$$

where

$$\begin{bmatrix} \xi_d(k+1) \\ \xi_q(k+1) \end{bmatrix} = \begin{bmatrix} \xi_d(k) \\ \xi_q(k) \end{bmatrix} + \begin{bmatrix} R & 0 \\ 0 & R \end{bmatrix} \begin{bmatrix} i_{d,ref}(k) - \hat{i}_d(k) \\ i_{q,ref}(k) - \hat{i}_q(k) \end{bmatrix} \quad (6)$$

and ω is grid angular frequency.

In order to compensate for the computational delay of one sampling period, $v_{Cfd}(k)$, $v_{Cfq}(k)$, $i_d(k)$, and $i_q(k)$ are estimated one sampling period ahead. The estimated state variables are denoted by $\hat{\cdot}$ in (4)–(6).

In case of unbalanced dips, control of positive- and negative-sequence components separately is required to obtain good control performance [13]. A controller for the negative-sequence components can be designed in a similar way as above. Note, however, that the negative sequence rotates opposite to the positive sequence and, consequently, the cross-coupling terms in the differential equations have opposite signs.

III. TRANSFER TO MICROGRID OPERATION DURING DIPS

In Fig. 4, a distributed generation system, which is connected through a power electronic converter to the grid, is shown. Further, a three-phase static transfer switch, which is inserted between the utility supply side and the load side, is shown. When a voltage dip occurs, the static transfer switch is opened to disconnect the load side, where sensitive equipment is located,

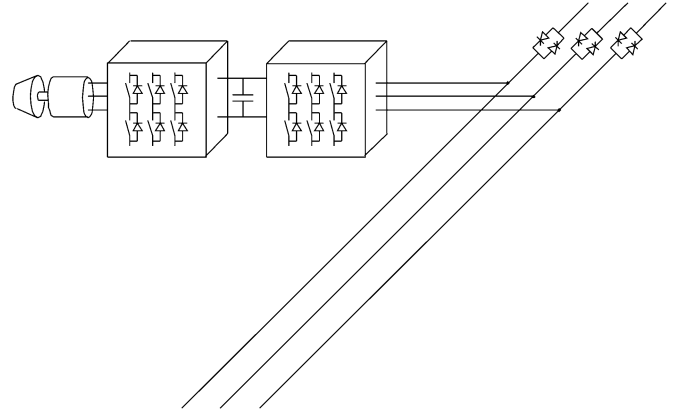


Fig. 4. A grid-interfaced distributed generation system which is isolated from the utility supply during dips by a static transfer switch.

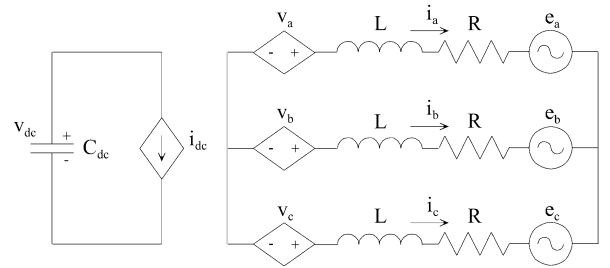


Fig. 5. Average model of a three-phase voltage-source inverter with L filter.

from the utility supply side. Typically, the static transfer switch comprises back-to-back thyristors. The distributed generation system at the load side regulates the voltage during the time that the loads are isolated from the utility supply. This is so-called (islanded) microgrid operation, referring to the concept introduced in [14]. In this way the operation of sensitive equipment is not affected by the voltage dips, assuming that the transfer between grid-connected operation and microgrid operation is seamless. During microgrid operation the distributed generation system supplies all the power needed by the loads. As soon as the supply voltage recovers, the static transfer switch is closed again and the distributed generation system is transferred from microgrid operation back to grid-connected operation. Attention should be paid that the voltage controlled by the distributed generation system and the supply voltage are synchronized before closing the switch [5].

The distributed generation system has to be designed for both grid-connected operation and microgrid operation. During grid-connected operation the converter controller of the distributed generation system regulates the current (i.e., current-mode control), whereas in microgrid operation, the controller regulates the voltage (i.e., voltage-mode control). The design of the controllers is covered in the following.

First, the controller in current-mode is developed. During grid-connected operation the inverter of the distributed generation system can be represented by the average model shown in Fig. 5. The output of the inverter is represented by the controlled voltage sources v_a , v_b , and v_c . The currents sourced into the grid phases a , b , and c are denoted by i_a , i_b , and i_c , respectively. Voltages e_a , e_b , and e_c represent the grid supply voltages. An L filter with inductance L and resistance R is

used to interface the converter output with the grid. Usually, an *LCL* filter is used for this purpose. However, at frequencies well below the resonance frequency of the *LCL* filter, as is the case here, this filter can be modeled as an inductance. The dc-bus voltage is v_{dc} and the dc current is i_{dc} .

The dynamics of the model in Fig. 5 are described by the following state-space equation in the *dq* reference frame:

$$\begin{aligned} \dot{x}(t) &= Ax(t) + Bu(t) + Ew(t) \\ y(t) &= Cx(t) \end{aligned} \quad (7)$$

where system, control, disturbance, and output matrices, respectively, are

$$\begin{aligned} A &= \begin{bmatrix} \frac{-R}{L} & \omega \\ -\omega & \frac{-R}{L} \end{bmatrix} \\ B &= \begin{bmatrix} \frac{1}{L} & 0 \\ 0 & \frac{1}{L} \end{bmatrix} \\ E &= \begin{bmatrix} \frac{-1}{L} & 0 \\ 0 & \frac{-1}{L} \end{bmatrix} \\ C &= \begin{bmatrix} 1 & 0 \\ 0 & 1 \end{bmatrix} \end{aligned}$$

and state, control, and disturbance vectors, respectively, are

$$\begin{aligned} x(t) &= [i_d(t) \quad i_q(t)]^T \\ u(t) &= [v_d(t) \quad v_q(t)]^T \\ w &= [e_d(t) \quad e_q(t)]^T. \end{aligned}$$

Again, as in the previous section, the controller is designed directly in discrete time. A forward difference approximation is applied, allowing (7) to be rewritten in a discrete-time form. Based on these approximated discrete-time equations, the control equations are obtained.

The controller that regulates the current during grid-connected operation, ensuring a deadbeat response, is given by

$$\begin{aligned} \begin{bmatrix} v_{d,ref}(k) \\ v_{q,ref}(k) \end{bmatrix} &= \begin{bmatrix} \frac{L}{T_s} + \frac{R}{2} & 0 \\ 0 & \frac{L}{T_s} + \frac{R}{2} \end{bmatrix} \begin{bmatrix} i_{d,ref}(k) - \hat{i}_d(k) \\ i_{q,ref}(k) - \hat{i}_q(k) \end{bmatrix} \\ &+ \begin{bmatrix} 0 & -\omega L & 1 & 0 \\ \omega L & 0 & 0 & 1 \end{bmatrix} \begin{bmatrix} \hat{i}_d(k) \\ \hat{i}_q(k) \\ e_d(k) \\ e_q(k) \end{bmatrix} \\ &+ \begin{bmatrix} \xi_d(k) \\ \xi_q(k) \end{bmatrix} \end{aligned} \quad (8)$$

where $\xi_d(k)$ and $\xi_q(k)$ are calculated in the same way as in (6).

Now, the voltage-mode control is developed. Since the average model, shown in Fig. 3, can be repeated to represent the inverter of the distributed generation system during microgrid operation, the same controller as given by (4)–(6) can be used.

IV. DIP DETECTION

It is very important that the time to detect a voltage dip is short in order to be able to quickly respond to it. Fast detection can be achieved with the algorithm given in [15]. This algorithm is adopted here. It is schematically represented in Fig. 6.

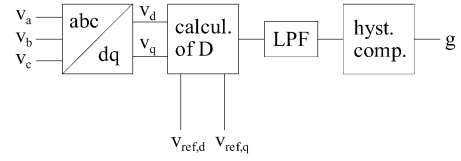


Fig. 6. Block diagram of voltage dip detection algorithm.

The utility voltage is measured and transformed to a *dq* reference frame. Then, the difference between the reference voltage and the measured voltage in the *dq* reference frame is calculated

$$\Delta V_d = V_{ref,d} - V_d \quad (9)$$

$$\Delta V_q = V_{ref,q} - V_q. \quad (10)$$

Further, (9) and (10) are combined as

$$|\Delta V| = \sqrt{\Delta V_d^2 + \Delta V_q^2}. \quad (11)$$

From (11), the signal D is calculated to express the deviation of the utility voltage from the given reference voltage as follows:

$$D = \frac{|\Delta V|}{\sqrt{V_{ref,d}^2 + V_{ref,q}^2}}. \quad (12)$$

This signal is used to detect the beginning and the end of a voltage dip. A low-pass filter is used to attenuate the ripple in the signal D , which is introduced in case of unbalanced dips. A moving average filter is used here. It has a settling time of a half cycle following any transient. The output of the filter is further processed by a dual hysteresis comparator. The lower and upper limits of the hysteresis comparator determine the sensitivity of the detection. The output signal g of the comparator is used to start or stop the series compensation or to open or close the static transfer switch.

V. TRANSIENT ANALYSIS

In this section, the response of both solutions to balanced and unbalanced dips is studied.

Simulation models for both suggested solutions have been developed to carry out the transient analysis. The software package Matlab/Simulink is used for the simulations.

The rms value of the supply voltage is 230 V and the grid frequency is 50 Hz. The parameters of the output filter of the series compensator are: $R = 0.05 \Omega$, $L = 6$ mH, and $C_f = 200 \mu\text{F}$. A sample period of $167 \mu\text{s}$ is used. The filter of the inverter in the microgrid solution has the following parameters: $R = 0.05 \Omega$, $L = 2$ mH, and $C_f = 15 \mu\text{F}$. The sample period is here $100 \mu\text{s}$.

A. Balanced Dips

First, both solutions are subjected to a balanced voltage dip of type A (for more details about dip classification, see [9]). The simulated dip in the supply voltage v_s is 40% and is shown in Fig. 7. The dip lasts from $t = 30$ ms to $t = 115$ ms. The recovery

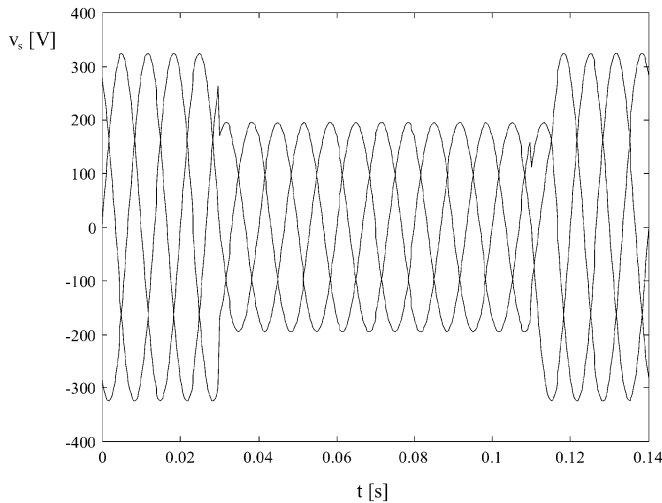


Fig. 7. Three-phase supply voltage during a dip of type A.

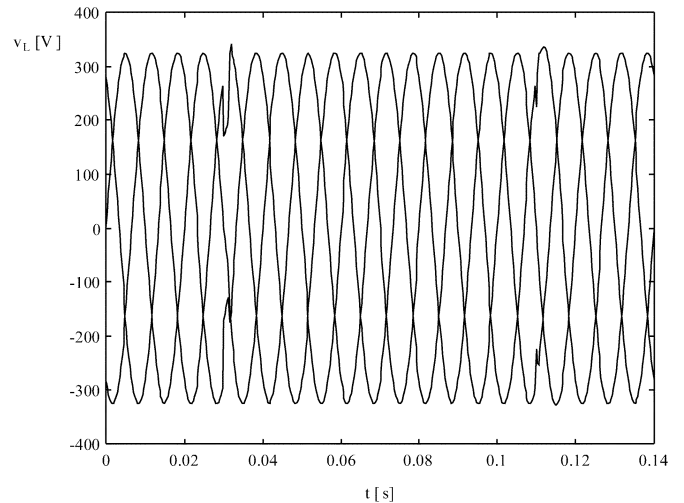


Fig. 9. Three-phase voltage at the load side (series compensation).

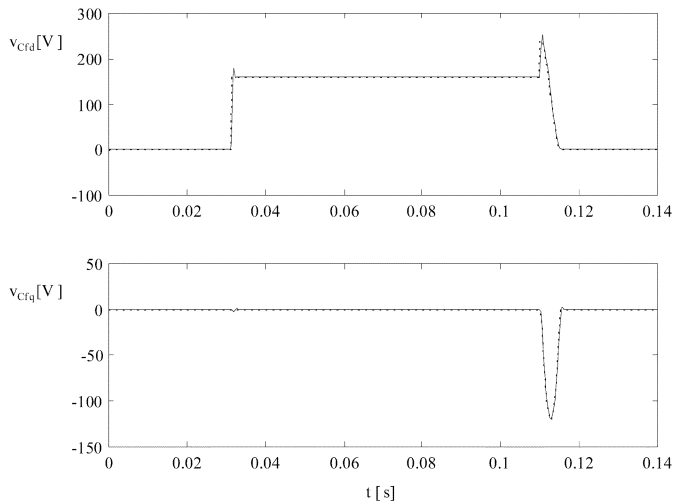


Fig. 8. d components (top) and q components (bottom) of the capacitor voltage (series compensation).

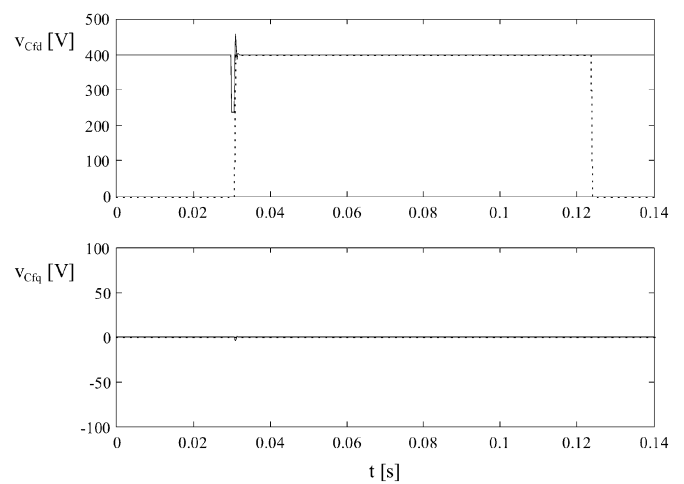


Fig. 10. d components (top) and q components (bottom) of the capacitor voltage (microgrid operation).

of the voltage is modeled according to the theory as described in [16].

Fig. 8 shows the dynamic response of the series compensator to this voltage dip. Both d and q components (solid curves) of the capacitor voltage, which is, of course, the injected voltage as seen earlier, are depicted. The d and q components of the desired reference values for the capacitor voltage (dotted curves) required to mitigate this dip are shown as well. It takes about 1 ms before the dip is detected and the series compensation starts. At $t = 110$ ms, the three-phase voltage dip develops into a two-phase voltage dip, which is reflected as an increase in both d and q components of the capacitor voltage. At $t = 123$ ms, the detection algorithm commands the series compensator to stop. The voltage v_L at the load side as a result of the series compensation is shown in Fig. 9. Clearly, this solution works effectively and the load voltage is barely affected by the dip.

Figs. 10 and 11 give the results for the case where the distributed generation system is transferred to microgrid operation during the voltage dip. The voltage across the capacitor in d and q components before, during, and after microgrid operation are given in Fig. 10. The voltage dip is detected at $t =$

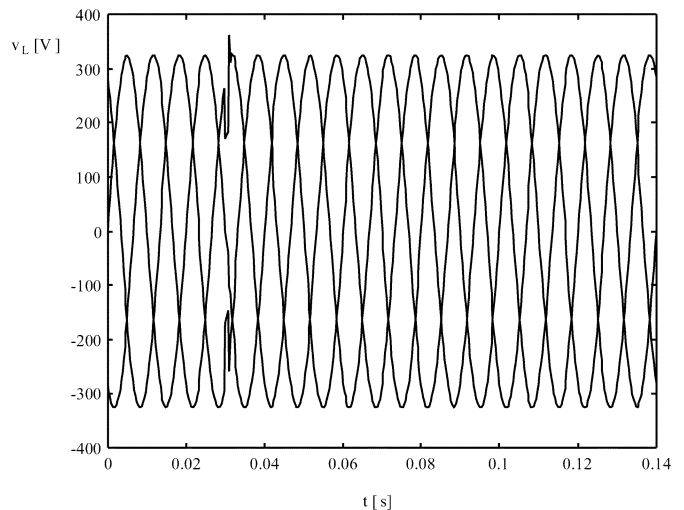


Fig. 11. Three-phase voltage at the load side (microgrid operation).

31 ms and after approximately 3 ms the static transfer switch is opened. The distributed generation system is then isolated from the utility supply. The controller operates now in voltage-

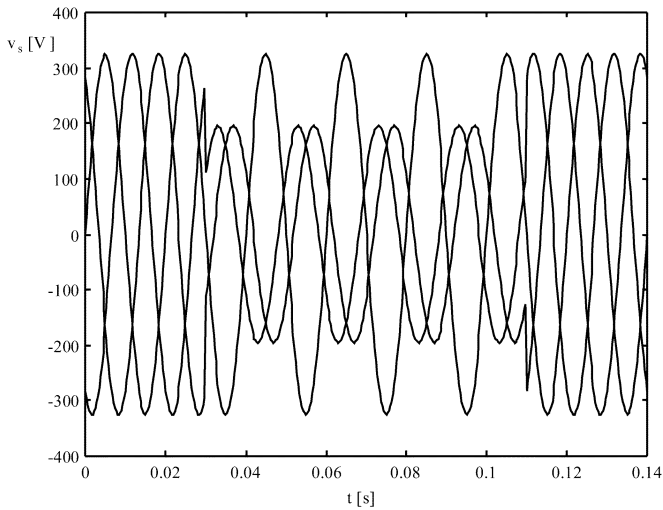


Fig. 12. Three-phase supply voltage during a dip of type C.

mode and regulates the voltage across the capacitor. This is the voltage to the sensitive equipment. The dotted curves show the d and q components of the reference values for the capacitor voltage during microgrid operation. After the voltage has completely recovered, the static transfer switch is closed again and the distributed generation system is reconnected to the utility supply. The controller operates in current-mode. It should be noted that, before closing the switch, the voltage controlled by the distributed generation system has to be in synchronism with the recovered supply voltage, as mentioned earlier. Fig. 11 illustrates how this solution manages to keep the voltage at the load side constant in the event of a voltage dip. Transition between grid-connected operation and microgrid operation and vice versa is seamless.

B. Unbalanced Dips

Now, the response to an unbalanced voltage dip is discussed. The simulated supply voltage affected by a dip of type C is shown in Fig. 12. The magnitude of the dip is 40%. The dip starts at $t = 30$ ms and ends at $t = 110$ ms.

Again, the series compensation is studied first. It is important to note that a negative-sequence controller is required to effectively mitigate an unbalanced voltage dip as seen in Section II. Therefore, the controller in the simulation model is modified in order to handle both positive- and negative-sequence components. The unbalanced voltage is decomposed in positive- and negative-sequence components according to the method applied in [13].

Figs. 13 and 14 show, respectively, the positive- and negative-sequence components of the injected voltage in the dq reference frame.

It also takes about 1 ms to detect this dip. The unbalanced voltage is decomposed in positive- and negative-sequence components in 5 ms. The compensation is stopped at $t = 120$ ms. The transient response is excellent, which is further illustrated by Fig. 15. The load voltage is nearly constant during the occurrence of the voltage dip.

The transient response for the microgrid solution during and after an unbalanced dip is shown in Figs. 16 and 17.

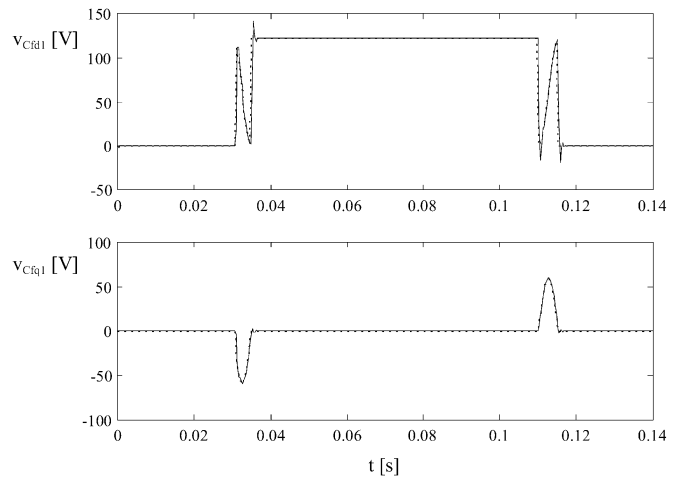


Fig. 13. Positive-sequence d components (top) and q components (bottom) of the capacitor voltage (series compensation).

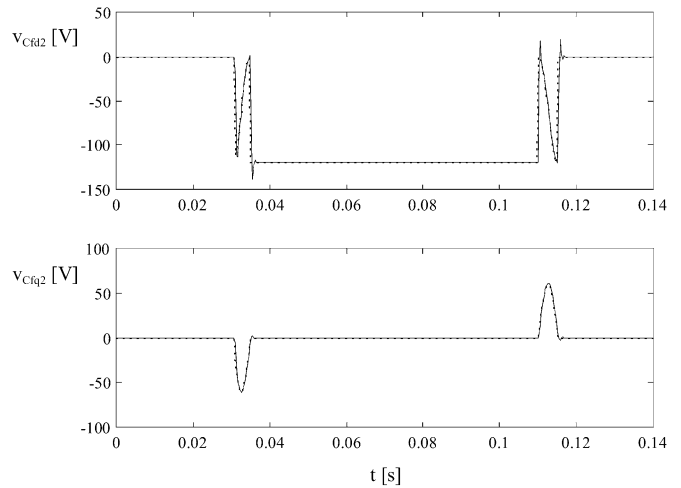


Fig. 14. Negative-sequence d components (top) and q components (bottom) of the capacitor voltage (series compensation).

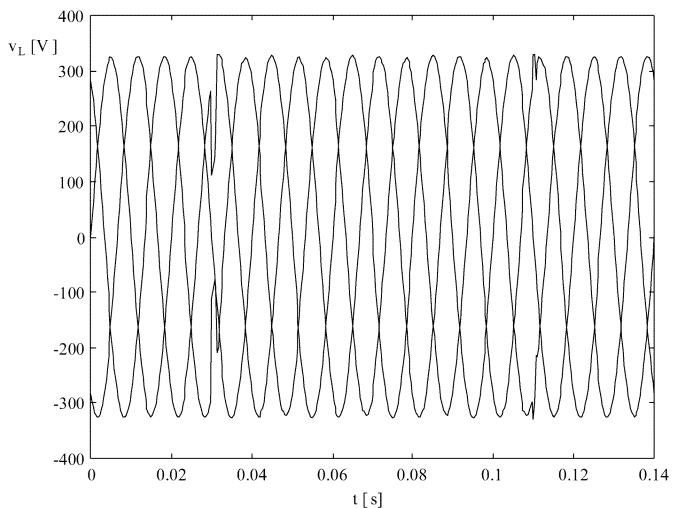


Fig. 15. Three-phase voltage at the load side (series compensation).

Also, for this solution, the transient response is very good. Fig. 16 shows the d and q components of the capacitor voltage, while Fig. 17 shows the voltage at the load side.

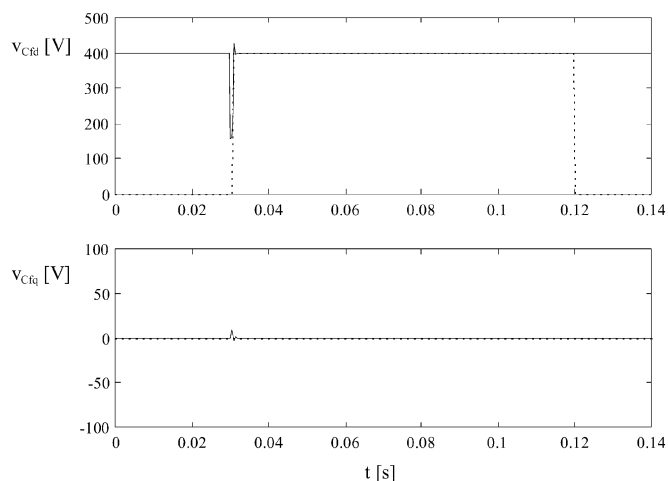


Fig. 16. d components (top) and q components (bottom) of the capacitor voltage (microgrid operation).

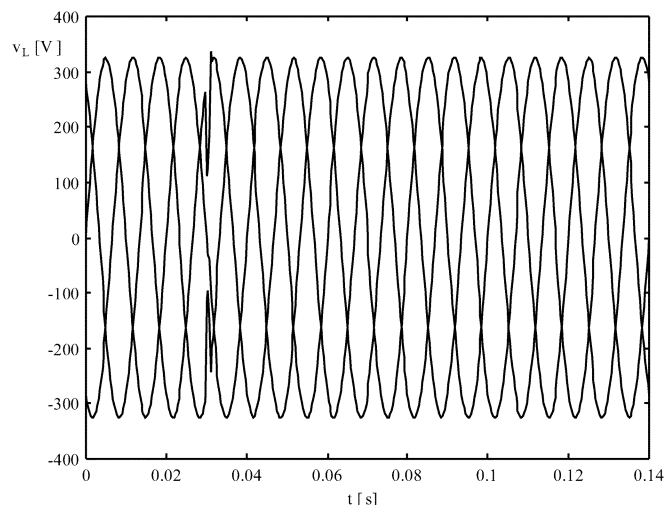


Fig. 17. Three-phase voltage at the load side (microgrid operation).

VI. CONCLUSION

This paper has covered the mitigation of voltage dips through distributed generation systems. Two possible ways to do so were presented, i.e., series compensation and transfer to microgrid operation during dips. The transient performance of both solutions was analyzed through simulations. Thereby, it was demonstrated that the dynamic response to voltage dips for both suggested solutions is comparable. It may be concluded that both solutions are very effective for mitigating voltage dips.

Series compensation can also be used to control the voltage in the event of other disturbances as well. By using appropriate control algorithms and sufficiently fast switching, the series compensator may be able to mitigate voltage transients, excessive voltage harmonics, and voltage fluctuations leading to light flicker. Series compensation can, however, not be used during interruptions and during voltage dips that exceed the rating of the series converter.

Microgrid operation can only be used during voltage dips and interruptions and its operation during voltage dips may be less

reliable than the series compensator. However, microgrid operation is probably the cheaper solution as the amount of power electronic components is clearly less.

REFERENCES

- [1] D. D. Sabin and A. Sundaram, "Quality enhances reliability," *IEEE Spectr.*, vol. 33, pp. 34–41, Feb. 1996.
- [2] V. E. Wagner, A. A. Andreshak, and J. P. Staniak, "Power quality and factory automation," *IEEE Trans. Ind. Applicat.*, vol. 26, pp. 620–626, July/Aug. 1990.
- [3] M. F. McGranaghan, D. R. Mueller, and M. J. S. Samotyj, "Voltage sags in industrial systems," *IEEE Trans. Ind. Applicat.*, vol. 29, pp. 397–403, Mar./Apr. 1993.
- [4] R. Tirumala, N. Mohan, and C. Henze, "Seamless transfer of grid-connected PWM inverters between utility-interactive and standalone modes," in *Proc. IEEE APEC'02*, 2002, pp. 1081–1086.
- [5] M. Illindala and G. Venkataramanan, "Control of distributed generation systems to mitigate load and line imbalances," in *Proc. IEEE PESC'02*, 2002, pp. 2013–2018.
- [6] W. E. Brumsickle, R. S. Schneider, G. A. Luckjiff, D. M. Divan, and M. F. McGranaghan, "Dynamic sag correctors: Cost-effective industrial power line conditioning," *IEEE Trans. Ind. Applicat.*, vol. 37, pp. 212–217, Jan./Feb. 2001.
- [7] A. Ghosh and G. Ledwich, "Compensation of distribution system voltage using DVR," *IEEE Trans. Power Delivery*, vol. 17, pp. 1030–1036, Oct. 2002.
- [8] P.-T. Cheng, C.-C. Huang, C.-C. Pan, and S. Bhattacharya, "Design and implementation of a series voltage sag compensator under practical utility conditions," in *Proc. IEEE APEC'02*, 2002, pp. 1061–1067.
- [9] M. H. J. Bollen, *Understanding Power Quality Problems, Voltage Sags and Interruptions*. Piscataway, NJ: IEEE Press, 1999.
- [10] N. Mohan, *Electric Drives: An Integrative Approach*. Minneapolis, MN: MNPERE, 2001.
- [11] D. Maksimović, A. M. Stanković, V. J. Thottuvelil, and G. C. Verghese, "Modeling and simulation of power electronic converters," *Proc. IEEE*, vol. 89, pp. 898–912, June 2001.
- [12] G. F. Franklin, J. D. Powell, and M. Workman, *Digital Control of Dynamic Systems*. Reading, MA: Addison-Wesley Longman, 1998.
- [13] H. Awad and J. Svensson, "Compensation of unbalanced voltage dips using vector-controlled static series compensator with LC-filter," in *Conf. Rec. IEEE-IAS Annu. Meeting*, 2002, pp. 904–910.
- [14] R. H. Lasseter, "MicroGrids," in *Proc. IEEE Power Eng. Soc. Winter Meeting*, 2002, pp. 305–308.
- [15] O. C. Montero-Hernández and P. N. Enjeti, "A fast detection algorithm suitable for mitigation of numerous power quality disturbances," in *Conf. Rec. IEEE-IAS Annu. Meeting*, 2001, pp. 2661–2666.
- [16] M. H. J. Bollen, "Voltage recovery after unbalanced and balanced voltage dips in three-phase systems," *IEEE Trans. Power Delivery*, vol. 18, pp. 1376–1381, Oct. 2003.



Koen J. P. Macken (M'02) received the M.Sc. degree from Eindhoven University of Technology, Eindhoven, The Netherlands, in 1996, and the Ph.D. degree from the Katholieke Universiteit Leuven, Leuven, Belgium, in 2003, both in electrical engineering.

He was a Visiting Scholar at the University of Manchester Institute of Science and Technology, Manchester, U.K., in 1995. He was with NK Cables (now part of Pirelli) and Delft University of Technology in The Netherlands between 1996–2000.

Since September 2000, he has been with the Katholieke Universiteit Leuven, where he is involved in research related to the use of renewable/distributed generation to enhance power quality. During the autumn of 2002, he was a Visiting Researcher at Chalmers University of Technology, Gothenburg, Sweden. His research interests include power electronics and electromagnetics.



Math H. J. Bollen (M'94–SM'96) received the M.Sc. and Ph.D. degrees from Eindhoven University of Technology, Eindhoven, The Netherlands, in 1985 and 1989, respectively.

He was a Researcher at Eindhoven University of Technology, a Lecturer at the University of Manchester Institute of Science and Technology, Manchester, U.K., and a Professor of electric power systems at Chalmers University of Technology, Gothenburg, Sweden. He is currently Coordinator of power quality and EMC with STRI AB, Ludvika,

Sweden. His research experience includes power quality and EMC, power system reliability, and power electronic applications to power systems.

Dr. Bollen is actively involved in IEEE, International Electrotechnical Commission, and CIGRE working groups on voltage dip analysis and statistics.



Ronnie J. M. Belmans (S'77–M'84–SM'89) received the M.Sc. and Ph.D. degrees in electrical engineering from the Katholieke Universiteit Leuven, Leuven, Belgium, in 1979 and 1984, respectively.

He is currently a Full Professor in the Department of Electrical Engineering, Katholieke Universiteit Leuven, where he teaches electrical energy systems, including electrical machines. He also serves as Chairman of the Board of Directors at the Belgian transmission system operator Elia. He has

been a Visiting Professor at McMaster University, Hamilton, ON, Canada, Rheinisch-Westfälische Technische Hochschule Aachen, Aachen, Germany, and Imperial College of Science, Technology and Medicine, London, U.K. His research interests include power quality, electrical energy systems, and electrical machine design.